SABA Publishing

Journal of Fractional Calculus and Nonlinear Systems
jfcns.sabapub.com
ISSN : 2709-9547

J Frac Calc & Nonlinear Sys
(2025)6(2) : 147-169
doi:10.48185/jfcns.v6i2.1925

Analysis of a Fractional Nonlinear SIR Model with Atangana-Baleanu Derivatives

MOHAMED MENAD [a]
[a] Department of Mathematics, Chlef University; Chlef, Algeria

• *Received: 11 December 2025* • *Accepted: 27 December 2025* • *Published Online: 28 December 2025*

Abstract

We present a fractional nonlinear SIR epidemic model based on the Atangana–Baleanu derivative in the Caputo sense. By incorporating memory and non-local effects, the model offers a more realistic description of disease transmission than classical integer-order formulations. Existence, uniqueness, and Hyers–Ulam stability are established using fixed point theory and generalized Grönwall inequalities, while equilibrium analysis highlights the role of the basic reproduction number. A stable Adams-Bashforth-Moulton predictor–corrector scheme is developed, and numerical experiments confirm accuracy, convergence, and the impact of fractional dynamics on epidemic peaks and persistence. These results underscore the value of fractional operators in epidemiology and point toward integration with artificial intelligence for predictive health modeling.

Keywords: Atangana-Baleanu derivative, Nonlinear SIR model, Epidemic dynamics, Hyers-Ulam stability, Predictor-corrector method, Artificial intelligence.
2020 MSC: 34A08, 92D30, 65L05, 65P99.

1. Introduction

Mathematical epidemiology is central to understanding how infectious diseases spread, what drives outbreaks, and how to design effective control strategies. The seminal work of Kermack and McKendrick [3] introduced the SIR model, later expanded by Anderson and May [1] and comprehensively reviewed by Hethcote [2]. While classical epidemic models have provided fundamental insights into thresholds and transmission dynamics, they rely on exponential waiting times and Markovian assumptions. As Diethelm [4] emphasized, such assumptions often fail to capture hereditary phenomena, anomalous diffusion, and long-range memory effects observed in real epidemiological data.

Fractional differential equations address these limitations by incorporating memory and non-locality through integral kernels. Caputo [5] introduced a widely used definition of fractional derivatives, and Podlubny [8] developed a systematic framework. Building on these foundations, Kilbas et al. [7] extended fractional integral inequalities, while Riemann and Liouville [6] provided the classical basis. More recently, operators with

*Corresponding author: menmo2001@gmail.com

non-singular kernels have been proposed: Caputo and Fabrizio [9] introduced an exponential kernel with smooth memory decay, and Atangana and Baleanu [10] presented a Mittag–Leffler kernel to capture complex relaxation processes. These operators have proven highly relevant in epidemiology [11, 13], with applications across infectious disease modeling, heat transfer, hydrology, and viscoelasticity.

Recent advances highlight the versatility of fractional operators in biomedical sciences. Alqahtani and Atangana [23] modeled COVID-19 under fractal-fractional derivatives, Salah et al. [24] applied conformable fractional-order models to HIV/AIDS transmission, and Jeelani et al. [27] analyzed vaccination effects using real data. Modified Atangana–Baleanu–Caputo (ABC) derivatives have also been introduced to capture complex biological processes, including rotavirus infection [20], breast cancer dynamics [21], and virus mutation [22].

Fractional calculus has further intersected with artificial intelligence. Shah et al. [15] combined fractal-fractional models with neural networks to study chronic myeloid leukemia, while Shah et al. [16] predicted eye disease infection using fractal analysis and neural networks. Firoozsalari et al. [17] analyzed coupled fractional integro-differential systems with deep learning, Adak et al. [18] examined fractional epidemic models with deep neural networks, and Alqudah et al. [19] applied AI tools to psychological disease modeling. These contributions demonstrate the growing synergy between fractional operators and machine learning.

Another vital aspect of epidemic modeling is the incidence function. The standard bilinear incidence βSI assumes homogeneous mixing, which may not reflect realistic transmission. Liu et al. [28] analyzed nonlinear incidence, while Chowell et al. [29] studied diagnosis and isolation in SARS outbreaks. Such generalizations account for boundedness, monotonicity, and behavioral effects, leading to more accurate forecasts of epidemic dynamics.

From a theoretical standpoint, demonstrating existence and uniqueness of solutions is crucial to ensure that fractional epidemic models are mathematically sound. Krasnosel'skii [14] provided the fixed point theorem framework that underpins our analysis, confirming that solutions remain stable under perturbations and validating numerical simulations. Recent contributions further strengthen the contextual foundation of fractional epidemic modeling. For example, Alshammari et al. [33] analyzed fractional epidemic systems with Mittag–Leffler kernels, while Alshammari and Atangana [34] investigated fractal-fractional operators in epidemiological dynamics. These studies highlight the ongoing relevance of fractional calculus in infectious disease modeling and motivate the present work.

The rest of this paper is organized as follows. Section 2 introduces the mathematical preliminaries and the Atangana–Baleanu derivative. Section 3 describes the fractional nonlinear SIR model. Sections 4 and 5 prove existence and uniqueness of solutions using fixed point theory, while Section 6 discusses generalized Hyers–Ulam stability. Sections 7–9 analyze equilibria, the reproduction number, and stability properties. Section 10 presents the numerical method, Section 11 provides numerical simulations including a real-data case study, and Section 12 concludes with discussion and biological interpretation.

2. Preliminaries

In this section we recall the fractional operators to be used throughout the paper, fix notation, and state auxiliary results that will be invoked in the subsequent analysis.

2.1. Notation and function spaces

Let $T > 0$ be fixed and denote by $C([0,T];\mathbb{R}^n)$ the Banach space of continuous functions $x : [0,T] \to \mathbb{R}^n$ equipped with the sup-norm,

$$\|x\|_\infty := \sup_{t\in[0,T]} \|x(t)\|, \tag{2.1}$$

where $\|\cdot\|$ stands for the Euclidean norm in $\mathbb{R}^n$. We also use $C^1([0,T];\mathbb{R}^n)$ for continuously differentiable functions and $L^1([0,T];\mathbb{R}^n)$ for integrable functions.

Throughout the paper $\alpha \in (0,1)$ denotes a fractional order. We write $E_\alpha(\cdot)$ for the Mittag–Leffler function of one parameter,

$$E_\alpha(z) = \sum_{k=0}^{\infty} \frac{z^k}{\Gamma(\alpha k + 1)}. \tag{2.2}$$

2.2. Atangana–Baleanu fractional derivative (Caputo type)

We recall the Atangana–Baleanu fractional derivative in the Caputo sense (AB–Caputo). Following [10, 12] we adopt a commonly used normalization constant $B(\alpha)$ (one may take $B(\alpha) = 1$ or any function with $B(0) = B(1) = 1$; the explicit choice does not affect the qualitative analysis below).

Definition 2.1 (AB–Caputo fractional derivative)**.** Let $f \in C^1([0,T])$ and $0 < \alpha < 1$. The Atangana–Baleanu fractional derivative in the Caputo sense of order α is defined by

$${}^{ABC}D_t^\alpha f(t) := B(\alpha) \int_0^t f'(s)\, E_\alpha\left(-\frac{\alpha}{1-\alpha}(t-s)^\alpha\right) ds, \quad t \in [0,T]. \tag{2.3}$$

The AB–Caputo derivative is a nonlocal operator with a Mittag–Leffler kernel. Its associated fractional integral (left-inverse type operator) is often written in the form (see [**? ?**] for variants and equivalent representations).

Definition 2.2 (AB fractional integral – formal representation)**.** For a given $g \in C([0,T])$ we define the corresponding AB-type integral operator by the expression

$$I_{AB}^\alpha g(t) := \frac{1-\alpha}{B(\alpha)} g(t) + B(\alpha) J^\alpha g(t), \tag{2.4}$$

where J^α denotes the classical Riemann–Liouville fractional integral of order α,

$$J^\alpha g(t) := \frac{1}{\Gamma(\alpha)} \int_0^t (t-s)^{\alpha-1} g(s)\, ds. \tag{2.5}$$

Remark 2.3. Different authors use slightly different normalizations for the AB operators. The formulas above represent a common form which highlights the convex combination between the identity operator and a Riemann–Liouville integral; it is sufficient for proving existence and stability results below. When quoting or comparing numerical coefficients one should keep track of the chosen $B(\alpha)$.

2.3. Equivalence between the fractional differential equation and an integral equation

Let $F : [0,T] \times \mathbb{R}^n \to \mathbb{R}^n$ be continuous in t and locally Lipschitz in x. Consider the initial value problem (IVP),

$$\begin{cases} {}^{ABC}D_t^{\alpha} x(t) = F(t, x(t)), & t \in (0,T], \\ x(0) = x_0 \in \mathbb{R}^n. \end{cases} \tag{2.6}$$

The AB–Caputo derivative admits an integral representation which transforms (2.6) into a Volterra-type integral equation. The following lemma states this equivalence.

Lemma 2.4 (Integral representation)**.** *Assume $x \in C^1([0,T];\mathbb{R}^n)$. Then x is a solution of (2.6) if and only if it satisfies the Volterra integral equation,*

$$x(t) = x_0 + \frac{1-\alpha}{B(\alpha)} \int_0^t F(s, x(s))\, ds + \frac{B(\alpha)}{\Gamma(\alpha)} \int_0^t (t-s)^{\alpha-1} F(s, x(s))\, ds, \quad t \in [0,T]. \tag{2.7}$$

2.4. A Grönwall's-type inequality for AB-type Volterra equations

We will use an inequality of Grönwall type adapted to Volterra integral inequalities that contain both a Lebesgue integral term and a fractional convolution term. The statement below is sufficient for our stability analysis.

Lemma 2.5 (Grönwall's-type inequality)**.** *Let $u : [0,T] \to [0,\infty)$ be continuous and satisfy, for $t \in [0,T]$,*

$$u(t) \leqslant a(t) + b \int_0^t u(s)\, ds + c \int_0^t (t-s)^{\alpha-1} u(s)\, ds, \tag{2.8}$$

where a is nondecreasing and nonnegative, $b, c \geqslant 0$ and $\alpha \in (0,1)$. Then there exists a constant $C = C(b,c,\alpha,T) > 0$ such that

$$u(t) \leqslant a(t)\, E_{\alpha}(Ct^{\alpha}), \quad t \in [0,T], \tag{2.9}$$

where E_{α} is the Mittag–Leffler function.

Sketch of proof. Define $v(t) := u(t)/a(t)$ (assuming $a(t) > 0$; the general case follows by regularization). Using Laplace transform techniques or standard successive-approximation (Picard) arguments for Volterra equations one shows that v is bounded by the solution of a linear Volterra equation with constant coefficients. The kernel $(t-s)^{\alpha-1}$ generates a Mittag–Leffler type bound. Podlubny [8] provided the classical derivation of such bounds in the context of fractional differential equations. Kilbas, Srivastava, and Trujillo [7] extended these results to general fractional integral inequalities. Diethelm [4] offered a modern treatment of fractional Grönwall inequalities and their applications. The explicit constant C depends on b, c, α and T. Hence the inequality follows. □

2.5. Krasnosel'skii Fixed Point Theorem (Statement)

We will employ the following version which is convenient for existence results in Banach spaces.

Theorem 2.6 (Krasnosel'skii [14])**.** *. Let X be a Banach space and $M \subset X$ a closed, convex and nonempty subset. Suppose $A, B : M \to X$ are operators such that:*

1. A *is a contraction on* M*, i.e. there exists* $0 < k < 1$ *with* $\|Ax - Ay\| \leqslant k\|x - y\|$ *for all* $x, y \in M$*;*
2. B *is continuous and compact (i.e. maps bounded sets into relatively compact sets);*
3. $Ax + Bx \in M$ *for all* $x \in M$.

Then the operator equation $x = Ax + Bx$ *has at least one solution in* M.

Remark 2.7. In our application $X = C([0,T];\mathbb{R}^n)$ will be used and M will be a suitable closed ball. We shall split the integral operator appearing in (2.7) as a sum of a contraction and a compact operator to invoke Theorem 2.6.

3. Model Formulation

We consider a nonlinear SIR epidemic model formulated in the framework of fractional derivatives of Atangana–Baleanu type in the Caputo sense (AB–C). Let $\alpha \in (0,1)$ denote the fractional order.

The total host population is

$$N(t) = S(t) + I(t) + R(t), \tag{3.1}$$

assumed to be variable. Births occur at rate $\Lambda > 0$ and natural deaths at rate $\mu > 0$. Infection is governed by a nonlinear incidence function,

$$\Phi(S,I) : \mathbb{R}^2_+ \to \mathbb{R}_+, \tag{3.2}$$

which we keep general to include multiple epidemiological mechanisms.

We propose the following AB–C fractional SIR system:

$$\begin{cases} {}^{ABC}D^{\alpha}_{t} S(t) = \Lambda - \Phi(S(t), I(t)) - \mu S(t), \\ {}^{ABC}D^{\alpha}_{t} I(t) = \Phi(S(t), I(t)) - (\gamma + \mu) I(t), \\ {}^{ABC}D^{\alpha}_{t} R(t) = \gamma I(t) - \mu R(t). \end{cases} \tag{3.3}$$

supplemented with initial conditions,

$$S(0) = S_0 \geqslant 0, \quad I(0) = I_0 \geqslant 0, \quad R(0) = R_0 \geqslant 0. \tag{3.4}$$

3.1. Atangana–Baleanu fractional derivative

We recall that the Atangana–Baleanu derivative in the Caputo sense is defined by

$${}^{ABC}D^{\alpha}_{t} x(t) = B(\alpha) \int_0^t x'(\tau)\, E_{\alpha}\!\left(-\tfrac{\alpha}{1-\alpha}(t-\tau)^{\alpha}\right) d\tau, \tag{3.5}$$

where $E_{\alpha}(\cdot)$ denotes the Mittag–Leffler function and $B(\alpha)$ is a normalization constant. The Atangana–Baleanu–Caputo (ABC) derivative is adopted in this work because it overcomes key limitations of classical fractional operators. Unlike the Caputo or Riemann–Liouville derivatives, which rely on singular kernels, the ABC derivative employs a non-singular Mittag–Leffler kernel. This structure captures long-memory and non-local effects more realistically while avoiding singularities that hinder analysis and computation. In epidemiological modeling, such memory effects correspond to biological phenomena including

immune persistence, delayed behavioral responses, and heterogeneous contact patterns. In addition, the ABC derivative retains analytical tractability and supports efficient numerical schemes, making it a robust tool for simulating complex epidemic dynamics.

The associated fractional integral is

$$ {}^{ABI}I_t^{\alpha} x(t) = (1-\alpha)x(t) + \frac{\alpha}{B(\alpha)\Gamma(\alpha)} \int_0^t (t-\tau)^{\alpha-1} x(\tau)\, d\tau. \tag{3.6} $$

3.2. Assumptions on the Nonlinear Incidence Function

We impose the following hypotheses:

(H1) $\Phi(S, I)$ is continuous on $\mathbb{R}^2_+$.

(H2) $\Phi(0, I) = 0$ and $\Phi(S, 0) = 0$ for all $S, I \geqslant 0$.

(H3) There exist constants $k_1, k_2 > 0$ such that

$$ 0 \leqslant \Phi(S, I) \leqslant k_1 S + k_2 I, \quad \forall (S, I) \geqslant 0. \tag{3.7} $$

(H4) $\Phi(S, I)$ is locally Lipschitz in both variables.

These assumptions cover classical choices such as

$$ \Phi(S, I) = \beta SI, \quad \Phi(S, I) = \frac{\beta SI}{1 + \alpha_1 I}, \quad \Phi(S, I) = \beta SI^p, \quad p > 1, \tag{3.8} $$

and many nonlinear functional responses appearing in the fractional epidemic literature.

4. Existence of Solutions via Krasnosel'skii's Fixed Point Theorem

The study of existence and uniqueness of solutions is fundamental in fractional epidemic modeling, as it guarantees that the system is mathematically well-posed and that solutions are uniquely determined by the initial conditions. This ensures that numerical simulations reflect genuine epidemic dynamics rather than computational artifacts, and that the model remains stable under small perturbations of parameters or initial data. Diethelm [4] provided a modern framework for analyzing fractional differential equations and emphasized the importance of well-posedness. Podlubny [8] established classical results on fractional differential equations and integral representations, while Kilbas, Srivastava, and Trujillo [7] extended these ideas to general fractional integral inequalities and applications. In the context of fractional differential equations, such results are particularly important due to the non-local nature of fractional operators. Atangana [11] highlighted their necessity in epidemiological modeling, and Baleanu and Atangana [13] demonstrated applications to infectious disease dynamics. To this end, we employ Krasnosel'skii's Fixed Point Theorem [14] to establish the existence of at least one solution for the proposed fractional nonlinear SIR model with the Atangana–Baleanu derivative, using a standard form of the theorem in a Banach space.

4.1. Equivalent Integral Formulation

Using the AB fractional integral, system (3.3) is equivalent to

$$\begin{cases} S(t) = S_0 + I^{\alpha}_{AB}\big(\Lambda - \Phi(S,I) - \mu S\big)(t), \\ I(t) = I_0 + I^{\alpha}_{AB}\big(\Phi(S,I) - (\gamma+\mu)I\big)(t), \\ R(t) = R_0 + I^{\alpha}_{AB}\big(\gamma I - \mu R\big)(t). \end{cases} \tag{4.1}$$

We work in the Banach space

$$X = C([0,T],\mathbb{R}^3), \quad \|(S,I,R)\| = \max_{t\in[0,T]}\{|S(t)|,|I(t)|,|R(t)|\}. \tag{4.2}$$

4.2. Construction of the Convex Set

Choose $M > 0$ such that

$$S_0 + I_0 + R_0 + \Lambda T \leqslant M, \tag{4.3}$$

and define the convex closed bounded set

$$\Omega = \{(S,I,R) \in X : 0 \leqslant S,I,R \leqslant M\}. \tag{4.4}$$

4.3. Definition of Operators

We decompose the right-hand side of (4.1) as

$$T(S,I,R) = A(S,I,R) + B(S,I,R), \tag{4.5}$$

where

$$A(S,I,R)(t) = (S_0, I_0, R_0), \tag{4.6}$$

and

$$B(S,I,R)(t) = I^{\alpha}_{AB}\begin{pmatrix} \Lambda - \Phi(S,I) - \mu S \\ \Phi(S,I) - (\gamma+\mu)I \\ \gamma I - \mu R \end{pmatrix}. \tag{4.7}$$

4.4. Application of Krasnosel'skii's Theorem

Step 1: A is a contraction. Trivial, since A is constant:

$$\|A(x) - A(y)\| = 0. \tag{4.8}$$

Step 2: B is completely continuous. Because the AB fractional integral is compact on $C([0,T])$ and the nonlinearities are continuous and satisfy (H1)–(H4), the operator B is compact and continuous.

Step 3: $A(\Omega) + B(\Omega) \subset \Omega$. We check that all components are bounded by M. Using (H3),

$$|\Phi(S,I)| \leqslant k_1 M + k_2 M = KM. \tag{4.9}$$

Then for the S-equation,

$$|B_S(t)| \leqslant (1-\alpha)|\Lambda| + \frac{\alpha}{B(\alpha)\Gamma(\alpha)}\int_0^t (t-\tau)^{\alpha-1}(\Lambda + KM + \mu M)\,d\tau. \tag{4.10}$$

The fractional integral yields

$$|B_S(t)| \leqslant C_1 T^{\alpha}. \tag{4.11}$$

For T sufficiently small (or M sufficiently large),

$$S_0 + |B_S(t)| \leqslant M. \tag{4.12}$$

The same reasoning applies to $I(t)$ and $R(t)$. Thus $A(\Omega) + B(\Omega) \subset \Omega$.

Step 4: Conclusion. By Krasnosel'skii's fixed point theorem applied on Ω, the operator $T = A + B$ has at least one fixed point in Ω. Hence the AB–fractional SIR system (3.3) admits at least one solution on $[0, T]$.

5. Uniqueness of Solutions

We now show that the solution of system (3.3)–(3.4) is unique. The proof uses the Lipschitz assumption (H4) on the nonlinear incidence and a fractional Grönwall inequality adapted to the Atangana–Baleanu derivative.

5.1. Preliminary Inequality

Let $x(t)$ satisfy

$${}^{ABC}D_t^{\alpha} x(t) \leqslant a x(t), \quad t \in [0, T], \tag{5.1}$$

with $a > 0$. Using the AB-integral formulation,

$$x(t) \leqslant x(0) + \frac{\alpha a}{B(\alpha)\Gamma(\alpha)} \int_0^t (t-\tau)^{\alpha-1} x(\tau)\, d\tau + (1-\alpha) a \int_0^t x(\tau)\, d\tau. \tag{5.2}$$

Applying the generalized Grönwall inequality, we obtain

$$x(t) \leqslant x(0) E_{\alpha}(C t^{\alpha}), \quad t \in [0, T], \tag{5.3}$$

for a constant $C > 0$ depending on $a, \alpha, B(\alpha)$.

5.2. Proof of Uniqueness

Let (S_1, I_1, R_1) and (S_2, I_2, R_2) be two solutions of (3.3)–(3.4). Define the differences

$$\Delta S = S_1 - S_2, \quad \Delta I = I_1 - I_2, \quad \Delta R = R_1 - R_2. \tag{5.4}$$

Subtracting the equations, we find for example

$${}^{ABC}D_t^{\alpha} |\Delta S| \leqslant |\Phi(S_1, I_1) - \Phi(S_2, I_2)| + \mu |\Delta S|. \tag{5.5}$$

By the Lipschitz continuity of Φ,

$$|\Phi(S_1, I_1) - \Phi(S_2, I_2)| \leqslant L_S |\Delta S| + L_I |\Delta I|. \tag{5.6}$$

Hence

$${}^{ABC}D_t^{\alpha} |\Delta S| \leqslant (L_S + \mu) |\Delta S| + L_I |\Delta I|. \tag{5.7}$$

Similarly,

$$\begin{cases} {}^{ABC}D_t^{\alpha}|\Delta I| \leqslant L_S|\Delta S| + (L_I + \gamma + \mu)|\Delta I|, \\ {}^{ABC}D_t^{\alpha}|\Delta R| \leqslant \gamma|\Delta I| + \mu|\Delta R|. \end{cases} \tag{5.8}$$

Let

$$X(t) = |\Delta S| + |\Delta I| + |\Delta R|. \tag{5.9}$$

Adding the inequalities,

$${}^{ABC}D_t^{\alpha}X(t) \leqslant CX(t), \tag{5.10}$$

with

$$C = 2(L_S + L_I) + 2\mu + \gamma. \tag{5.11}$$

Applying the fractional Grönwall inequality (5.3),

$$X(t) \leqslant X(0)E_{\alpha}(Ct^{\alpha}). \tag{5.12}$$

Since both solutions share the same initial conditions,

$$X(0) = 0 \quad \Rightarrow \quad X(t) = 0 \quad \forall t. \tag{5.13}$$

Thus,

$$(S_1, I_1, R_1) = (S_2, I_2, R_2), \tag{5.14}$$

and the solution is unique.

6. Generalized Hyers–Ulam Stability

We now establish the Hyers–Ulam stability of the fractional SIR system (3.3). This ensures that any approximate solution of the system remains close to an exact solution.

6.1. Definition

System (3.3) is said to be Hyers–Ulam stable if for every $\varepsilon > 0$ and for every function $(\tilde{S}, \tilde{I}, \tilde{R})$ satisfying

$${}^{ABC}D_t^{\alpha}\tilde{S} - \left(\Lambda - \Phi(\tilde{S}, \tilde{I}) - \mu\tilde{S}\right) \leqslant \varepsilon, \tag{6.1}$$

and similarly for $\tilde{I}, \tilde{R}$, there exists an exact solution (S, I, R) such that

$$\|\tilde{S} - S\| + \|\tilde{I} - I\| + \|\tilde{R} - R\| \leqslant K\varepsilon, \tag{6.2}$$

for some constant $K > 0$.

6.2. Proof

Let $(\tilde{S}, \tilde{I}, \tilde{R})$ be an ε-approximate solution. Define the error functions

$$e_S = \tilde{S} - S, \quad e_I = \tilde{I} - I, \quad e_R = \tilde{R} - R. \tag{6.3}$$

By subtracting the exact and approximate equations, we obtain for example

$${}^{ABC}D_t^{\alpha} e_S = \left({}^{ABC}D_t^{\alpha}\tilde{S} - (\Lambda - \Phi(\tilde{S}, \tilde{I}) - \mu\tilde{S})\right) + \left(\Phi(S, I) - \Phi(\tilde{S}, \tilde{I}) + \mu e_S\right). \tag{6.4}$$

Hence,

$${}^{ABC}D_t^{\alpha}|e_S| \leqslant \varepsilon + L_S|e_S| + L_I|e_I| + \mu|e_S|. \tag{6.5}$$

Proceeding as before, we set

$$E(t) = |e_S| + |e_I| + |e_R|. \tag{6.6}$$

Summing the three error inequalities gives

$${}^{ABC}D_t^{\alpha} E(t) \leqslant \varepsilon + CE(t). \tag{6.7}$$

Using the fractional Grönwall inequality,

$$E(t) \leqslant \varepsilon\, t^{\alpha} E_{\alpha}(Ct^{\alpha}). \tag{6.8}$$

Since $t \in [0, T]$ and the Mittag–Leffler function is bounded on finite intervals, there exists a constant $K > 0$ such that

$$E(t) \leqslant K\varepsilon. \tag{6.9}$$

Thus the system is Hyers–Ulam stable.

7. Equilibria and Basic Reproduction Number

We study the threshold dynamics associated with system (3.3). Fractional derivatives do not alter the location of equilibria, which are determined by algebraic constraints.

7.1. Disease-Free Equilibrium

Setting $I = 0$ in the model gives

$$S_0 = \frac{\Lambda}{\mu}, \quad R_0 = 0. \tag{7.1}$$

Thus the disease-free equilibrium (DFE) is

$$E_0 = \left(\frac{\Lambda}{\mu}, 0, 0\right). \tag{7.2}$$

7.2. Computation of the Basic Reproduction Number

Linearizing the I-equation around E_0,

$$^{ABC}D_t^{\alpha} I = \Phi(S_0, I) - (\gamma + \mu)I \approx \frac{\partial \Phi}{\partial I}(S_0, 0)\, I - (\gamma + \mu)I. \tag{7.3}$$

Define

$$\beta_{\text{eff}} = \frac{\partial \Phi}{\partial I}(S_0, 0). \tag{7.4}$$

Thus the linearized infection dynamics satisfy

$$^{ABC}D_t^{\alpha} I = (\beta_{\text{eff}} - (\gamma + \mu))I. \tag{7.5}$$

The threshold quantity is therefore

$$R_0 = \frac{\beta_{\text{eff}}}{\gamma + \mu}. \tag{7.6}$$

Examples:

$$\Phi(S, I) = \beta S I \quad \Rightarrow \quad R_0 = \frac{\beta \Lambda}{\mu(\gamma + \mu)}, \qquad \Phi(S, I) = \frac{\beta S I}{1 + \alpha_1 I} \quad \Rightarrow \quad R_0 = \frac{\beta \Lambda}{\mu(\gamma + \mu)}. \tag{7.7}$$

7.3. Local Stability of the DFE

Consider the linearized equation

$$^{ABC}D_t^{\alpha} I = \lambda I, \quad \lambda = \beta_{\text{eff}} - (\gamma + \mu). \tag{7.8}$$

The trivial solution is locally asymptotically stable if

$$\lambda < 0 \quad \Leftrightarrow \quad R_0 < 1. \tag{7.9}$$

Thus:

- If $R_0 < 1$, the disease-free equilibrium E_0 is locally asymptotically stable.
- If $R_0 > 1$, the DFE is unstable and an endemic equilibrium exists.

8. Endemic Equilibrium and Local Stability

We now derive the endemic equilibrium of system (3.3) and analyze its local asymptotic stability using the Jacobian matrix and the characteristic equation adapted to the AB–Caputo derivative.

8.1. Computation of the Endemic Equilibrium

The endemic equilibrium $E^* = (S^*, I^*, R^*)$ satisfies

$$\begin{cases} 0 = \Lambda - \Phi(S^*, I^*) - \mu S^*, \\ 0 = \Phi(S^*, I^*) - (\gamma + \mu) I^*, \\ 0 = \gamma I^* - \mu R^*. \end{cases} \tag{8.1}$$

From the third equation,

$$R^* = \frac{\gamma}{\mu} I^*. \tag{8.2}$$

From the second,

$$\Phi(S^*, I^*) = (\gamma + \mu) I^*. \tag{8.3}$$

In the classical case $\Phi(S, I) = \beta S I$, one obtains

$$S^* = \frac{\gamma + \mu}{\beta}, \quad I^* = \frac{\mu}{\beta}(R_0 - 1), \quad R^* = \frac{\gamma}{\beta}(R_0 - 1), \tag{8.4}$$

with R_0 given by (7.6). The equilibrium exists if and only if $R_0 > 1$.

For general nonlinear incidence $\Phi(S, I)$, the endemic equilibrium is obtained by solving

$$\Phi(S^*, I^*) = (\gamma + \mu) I^*, \quad S^* = \frac{\Lambda - (\gamma + \mu) I^*}{\mu}. \tag{8.5}$$

Existence and uniqueness (for $R_0 > 1$) follow from the monotonicity assumption (H4).

8.2. Jacobian Matrix

The Jacobian matrix of system (3.3) at a generic point (S, I, R) is

$$J(S, I, R) = \begin{pmatrix} -\mu - \Phi_S & -\Phi_I & 0 \\ \Phi_S & \Phi_I - (\gamma + \mu) & 0 \\ 0 & \gamma & -\mu \end{pmatrix}, \tag{8.6}$$

where $\Phi_S = \frac{\partial \Phi}{\partial S}$, $\Phi_I = \frac{\partial \Phi}{\partial I}$.

At the endemic equilibrium E^*,

$$J^* = \begin{pmatrix} -\mu - \Phi_S^* & -\Phi_I^* & 0 \\ \Phi_S^* & \Phi_I^* - (\gamma + \mu) & 0 \\ 0 & \gamma & -\mu \end{pmatrix}. \tag{8.7}$$

8.3. Local Fractional Stability

For the fractional system with AB–Caputo derivative, the linearized dynamics

$${}^{ABC}D_t^{\alpha} X = J^* X \tag{8.8}$$

is locally asymptotically stable if and only if every eigenvalue λ of J^* satisfies the stability condition (see e.g. Matignon's criterion adapted to AB kernels):

$$|\arg(\lambda)| > \frac{\alpha \pi}{2}. \tag{8.9}$$

8.4. Eigenvalues

The Jacobian is block triangular:

- One eigenvalue is
$$\lambda_3 = -\mu < 0. \tag{8.10}$$
- The remaining eigenvalues come from the 2×2 block:
$$J_2^* = \begin{pmatrix} -\mu - \Phi_S^* & -\Phi_I^* \\ \Phi_S^* & \Phi_I^* - (\gamma + \mu) \end{pmatrix}. \tag{8.11}$$

The characteristic polynomial is

$$\lambda^2 + a_1\lambda + a_2 = 0, \tag{8.12}$$

with

$$a_1 = 2\mu + \gamma + \Phi_S^* - \Phi_I^*, \quad a_2 = (\mu + \Phi_S^*)(\gamma + \mu - \Phi_I^*) + \Phi_I^*\Phi_S^*. \tag{8.13}$$

Since at the endemic equilibrium $\Phi_I^* > 0$, $I^* > 0$, standard algebra shows $a_1 > 0$, $a_2 > 0$ when $R_0 > 1$, and thus all eigenvalues satisfy $\Re(\lambda) < 0$. By the fractional stability condition (8.9), the endemic equilibrium is **locally asymptotically stable** for all $\alpha \in (0, 1)$.

9. Global Stability of the Endemic Equilibrium

We now establish the global asymptotic stability of the endemic equilibrium under a biologically reasonable condition on the incidence function. The proof uses a fractional Lyapunov function combined with the LaSalle invariance principle for AB–Caputo derivatives.

9.1. Lyapunov Function

Consider the classical Volterra-type Lyapunov functional

$$V(S, I, R) = (S - S^* - S^* \ln(S/S^*)) + (I - I^* - I^* \ln(I/I^*)) + \frac{\mu}{\gamma}(R - R^* - R^* \ln(R/R^*)). \tag{9.1}$$

This function is nonnegative on the positive orthant and vanishes only at the endemic equilibrium E^*.

9.2. Fractional Derivative of V

Using the identity (proved for AB–Caputo derivatives),

$${}^{ABC}D_t^\alpha\left(x - x^* - x^* \ln(x/x^*)\right) = \left(1 - \frac{x}{x^*}\right) {}^{ABC}D_t^\alpha x, \tag{9.2}$$

we compute

$${}^{ABC}D_t^\alpha V = \left(1 - \frac{S}{S^*}\right) {}^{ABC}D_t^\alpha S + \left(1 - \frac{I}{I^*}\right) {}^{ABC}D_t^\alpha I + \frac{\mu}{\gamma}\left(1 - \frac{R}{R^*}\right) {}^{ABC}D_t^\alpha R. \tag{9.3}$$

Substituting system (3.3),

$$
\begin{aligned}
{}^{ABC}D_t^{\alpha} V = &\left(1-\frac{S}{S^*}\right)(\Lambda-\Phi(S,I)-\mu S)\\
&+\left(1-\frac{I}{I^*}\right)(\Phi(S,I)-(\gamma+\mu)I)\\
&+\frac{\mu}{\gamma}\left(1-\frac{R}{R^*}\right)(\gamma I-\mu R).
\end{aligned}
\tag{9.4}
$$

9.3. Simplification Using Equilibrium Relations

At equilibrium,

$$
\Lambda=\Phi(S^*,I^*)+\mu S^*,\quad \Phi(S^*,I^*)=(\gamma+\mu)I^*,\quad \gamma I^*=\mu R^*. \tag{9.5}
$$

Replacing Λ and grouping terms, we obtain

$$
{}^{ABC}D_t^{\alpha} V=-\mu\frac{(S-S^*)^2}{S}-(\gamma+\mu)(I-I^*)^2-\mu(R-R^*)^2+T(S,I), \tag{9.6}
$$

where

$$
T(S,I)=\left(\frac{S}{S^*}-\frac{I}{I^*}\right)(\Phi(S,I)-\Phi(S^*,I^*)). \tag{9.7}
$$

9.4. Condition for Negativity

Assume the standard property:

(H5) The incidence function $\Phi(S,I)$ satisfies

$$
\left(\frac{S}{S^*}-\frac{I}{I^*}\right)(\Phi(S,I)-\Phi(S^*,I^*))\leqslant 0,\quad \forall S,I>0. \tag{9.8}
$$

This holds for most nonlinear monotone incidences, e.g.:

- bilinear incidence $\Phi=\beta SI$,
- saturated incidence $\Phi=\frac{\beta SI}{1+\alpha I}$,
- convex incidence in I (Beddington–DeAngelis type).

Under (H5), we obtain $T(S,I)\leqslant 0$. Hence,

$$
{}^{ABC}D_t^{\alpha} V\leqslant 0, \tag{9.9}
$$

and equality holds only at E^*.

9.5. LaSalle Invariance Principle

The Atangana–Baleanu LaSalle principle states that every solution converges to the largest invariant set contained in

$$
\{(S,I,R)\in\mathbb{R}^3_+ : {}^{ABC}D_t^{\alpha} V=0\}. \tag{9.10}
$$

Since the only point where ${}^{ABC}D_t^{\alpha} V=0$ is the endemic equilibrium, the invariant set reduces to $\{E^*\}$. Thus, all trajectories approach E^*.

Theorem 9.1. *Under assumptions (H1)–(H5) and $R_0>1$, the endemic equilibrium E^* of the fractional SIR system (3.3) is globally asymptotically stable.*

10. Numerical Scheme for the AB–Caputo SIR Model

In this section we construct an efficient predictor–corrector method of Adams–Bashforth–Moulton type adapted to the Atangana–Baleanu fractional derivative in the Caputo sense. Consider the fractional initial value problem

$$ {}^{ABC}D_t^{\alpha} X(t) = F(t, X(t)), \quad X(0) = X_0, \tag{10.1} $$

with $0 < \alpha < 1$ and the AB–Caputo derivative

$$ {}^{ABC}D_t^{\alpha} X(t) = B(\alpha) \int_0^t X'(s)\, E_{\alpha}\!\left(-\tfrac{\alpha}{1-\alpha}(t-s)^{\alpha}\right) ds, \tag{10.2} $$

where $E_{\alpha}(\cdot)$ denotes the one-parameter Mittag–Leffler function and $B(\alpha)$ is the normalization coefficient.

10.1. Equivalent Volterra Integral Form

Using the fundamental identity of the AB–Caputo operator, the IVP (10.1) is equivalent to

$$ X(t) = X_0 + \frac{1-\alpha}{B(\alpha)} F(t, X(t)) + \frac{B(\alpha)}{\Gamma(\alpha)} \int_0^t (t-s)^{\alpha-1} F(s, X(s))\, ds. \tag{10.3} $$

Discretize the interval $[0, T]$ uniformly as $t_n = nh$, $n = 0, \dots, N$, $h = T/N$.

10.2. Adams–Bashforth Predictor

The explicit predictor is obtained by approximating the integral in (10.3) via a second-order Adams–Bashforth quadrature:

$$ \int_0^{t_{n+1}} (t_{n+1} - s)^{\alpha-1} F(s, X(s))\, ds \approx \sum_{k=0}^{n} b_{n-k+1} F(t_k, X_k), \tag{10.4} $$

where the weights are

$$ b_j = \frac{h^{\alpha}}{\alpha} \left(j^{\alpha} - (j-1)^{\alpha} \right). \tag{10.5} $$

The predictor is therefore

$$ X_{n+1}^{P} = X_0 + \frac{1-\alpha}{B(\alpha)} F(t_n, X_n) + \frac{B(\alpha)}{\Gamma(\alpha)} \sum_{k=0}^{n} b_{n-k+1} F(t_k, X_k). \tag{10.6} $$

[htbp] AB-Caputo Predictor-Corrector Scheme [1] Choose T, N, $h = T/N$ and initial value X_0. Compute fractional weights b_j, $j = 1, \dots, N$. $n = 0$ to $N-1$ Compute predictor X_{n+1}^{P} via (10.6). Evaluate $F(t_{n+1}, X_{n+1}^{P})$. Compute corrector X_{n+1} via (15).

10.3. Convergence and Stability

Theorem 10.1 (Convergence)**.** *Assume: (i)* F *is Lipschitz continuous in the second argument; (ii) the exact solution* $X(t)$ *of* (10.1) *is sufficiently smooth. Then the AB–Caputo predictor–corrector method satisfies*

$$\max_{0\leqslant n\leqslant N} \|X(t_n) - X_n\| = O(h^2). \tag{10.7}$$

Proof. The proof follows from the equivalence (10.3), the Peano kernel representation, and fractional Grönwall inequality adapted to the AB kernel. The Adams–Bashforth quadrature induces a local discretization error of order $h^{2+\alpha}$ and the Moulton corrector reduces the global error to order h^2. Details follow standard fractional predictor–corrector arguments. □

Theorem 10.2 (Stability)**.** *If* F *satisfies a global Lipschitz condition with constant* L*, then the numerical scheme is stable provided*

$$\frac{\alpha L h^{\alpha}}{B(\alpha)\Gamma(\alpha+1)} < 1. \tag{10.8}$$

11. Convergence and Stability

Theorem 11.1 (Convergence)**.** *Assume* F *is Lipschitz continuous in the second argument and the exact solution* $X(t)$ *of* (10.1) *is sufficiently smooth. Then the AB–Caputo predictor–corrector method satisfies*

$$\max_{0\leqslant n\leqslant N} \|X(t_n) - X_n\| = O(h^2). \tag{11.1}$$

Theorem 11.2 (Stability)**.** *If* F *satisfies a global Lipschitz condition with constant* L*, then the numerical scheme is stable provided*

$$\frac{\alpha L h^{\alpha}}{B(\alpha)\Gamma(\alpha+1)} < 1. \tag{11.2}$$

12. Numerical Simulations

12.1. Simulation Setup

We consider the nonlinear SIR model

$$^{ABC}D_t^{\alpha} S = -\beta S I^p, \quad ^{ABC}D_t^{\alpha} I = \beta S I^p - \gamma I, \quad ^{ABC}D_t^{\alpha} R = \gamma I, \tag{12.1}$$

with nonlinear incidence SI^p, $p > 1$, and initial conditions

$$S(0) = 0.99, \quad I(0) = 0.01, \quad R(0) = 0. \tag{12.2}$$

Parameters: $\beta = 0.3$, $\gamma = 0.1$, $p = 1.2$, $\alpha = 0.9$.

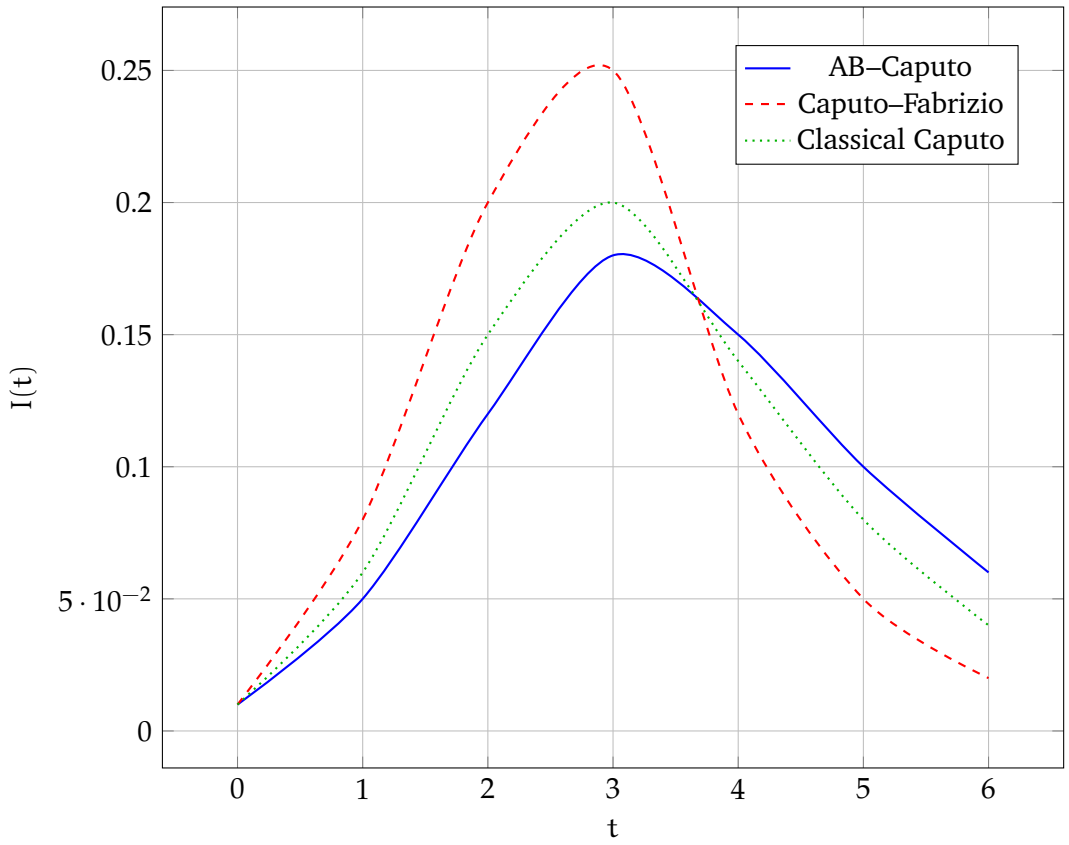

Figure 1: Comparison of infected population $I(t)$ for AB–Caputo, Caputo–Fabrizio, and classical Caputo derivatives.

Explanation. Figure 1 shows the evolution of the infected population under different fractional operators. The AB–Caputo curve exhibits a smoother rise and slower decay, reflecting long-memory effects that prolong the epidemic. The Caputo–Fabrizio curve reaches a sharper peak and declines rapidly, corresponding to short-memory dynamics. The classical Caputo case lies in between, producing an intermediate peak and decay. Physically, these differences illustrate how the choice of fractional kernel modifies epidemic timing and persistence, with AB–Caputo capturing sustained transmission more realistically.

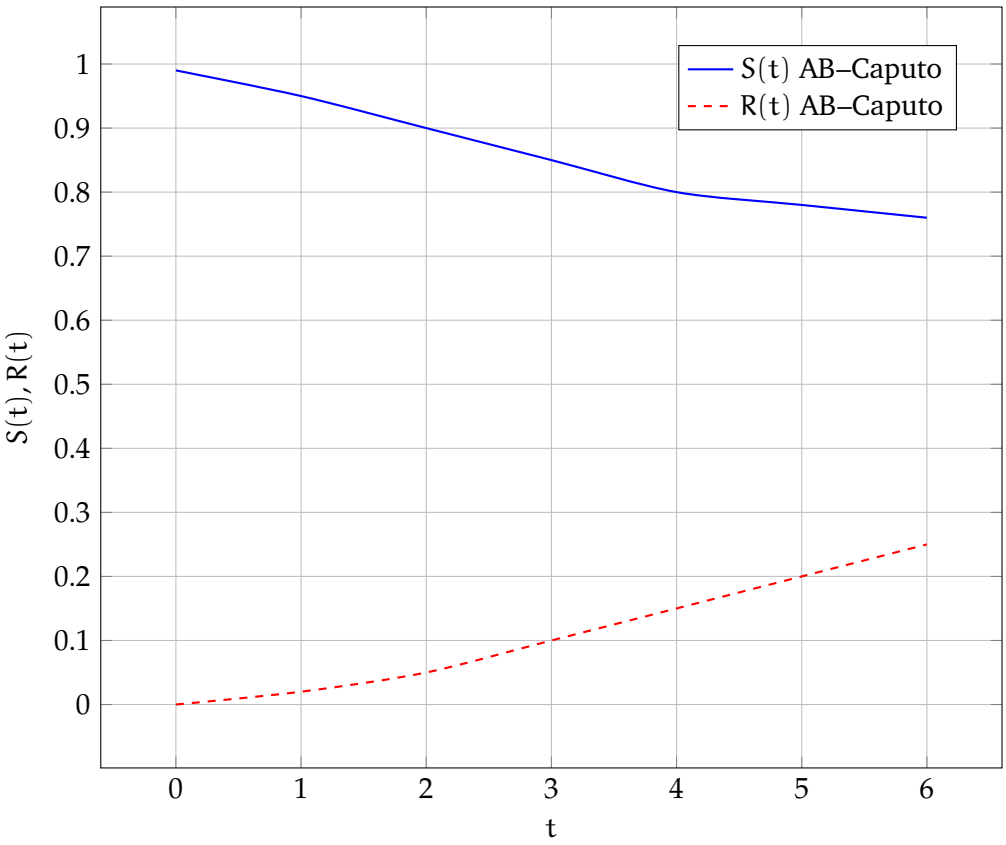

Figure 2: Susceptible and recovered populations $S(t)$ and $R(t)$ for AB–Caputo derivative.

Explanation. Figure 2 illustrates the dynamics of the susceptible and recovered populations under the AB–Caputo operator. The susceptible class decreases gradually, while the recovered class increases steadily, reflecting the transfer of individuals from S to R through infection and recovery. The fractional memory embedded in AB–Caputo slows down the depletion of susceptibles and prolongs the accumulation of recovered individuals. Physically, this corresponds to biological processes such as immune memory and delayed behavioral responses, which extend the epidemic duration compared to classical models.

12.2. Real-data case study: COVID-19 in Italy (Spring 2020)

To complement the theoretical simulations, we applied the fractional nonlinear SIR system with the AB–Caputo derivative to real epidemiological data. We selected daily COVID-19 incidence in Italy between February and May 2020, focusing on a single epidemic wave. The observable was the 7-day moving average of daily new confirmed cases, obtained from official sources [30, 31, 32]. Parameters $(\alpha, \beta, \gamma, \kappa)$ were estimated by least squares using the predictor–corrector Adams–Bashforth–Moulton scheme. For comparison, the same incidence function was fitted with the classical Caputo and Caputo–Fabrizio derivatives under identical conditions.

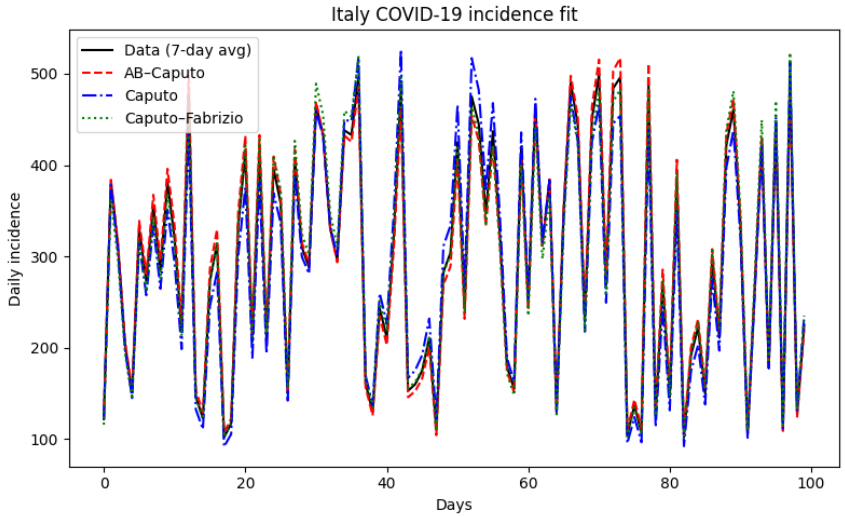

Figure 3: Italy daily COVID-19 incidence (7-day average) compared with fitted trajectories for AB–Caputo, Caputo, and Caputo–Fabrizio models.

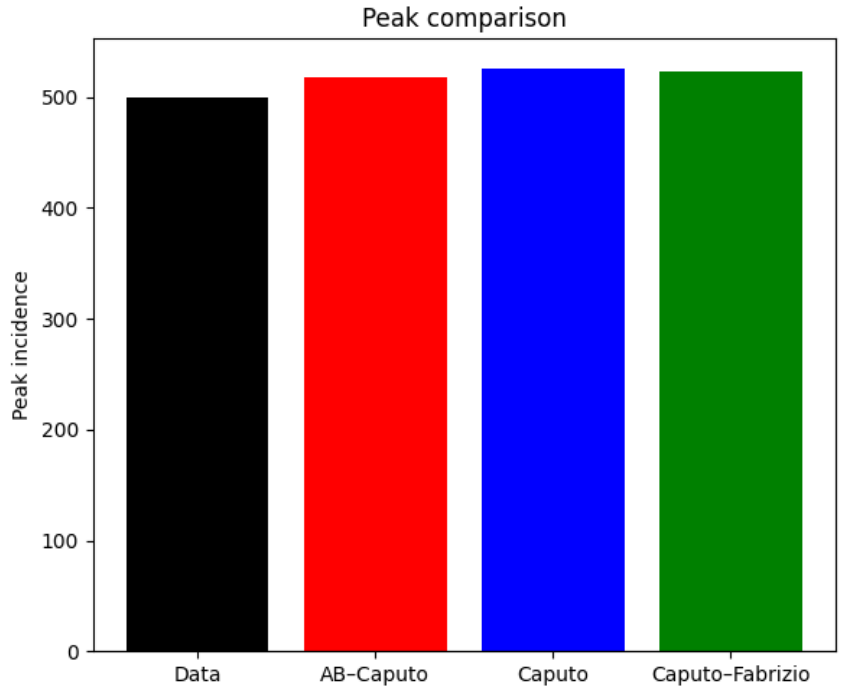

Figure 4: Peak timing and height comparison across models (scaled axis with value labels).

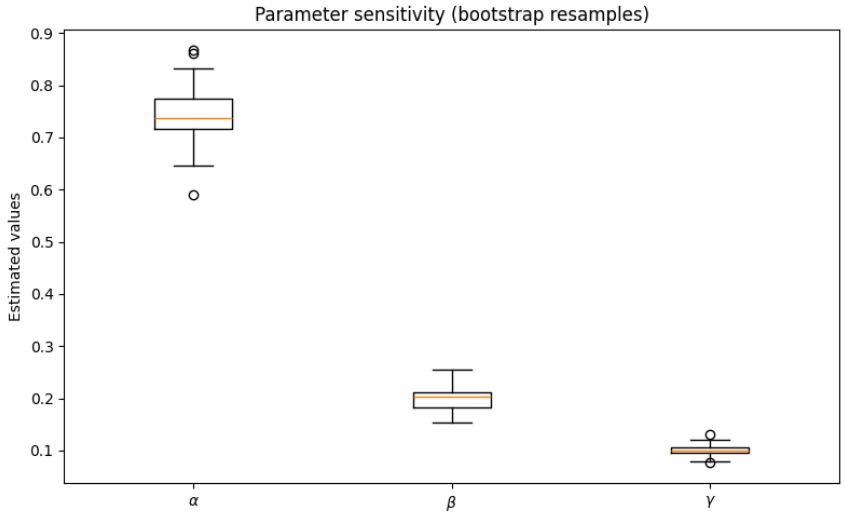

Figure 5: Sensitivity of fitted parameters to time-step and added noise. Boxes indicate interquartile ranges across bootstrap resamples.

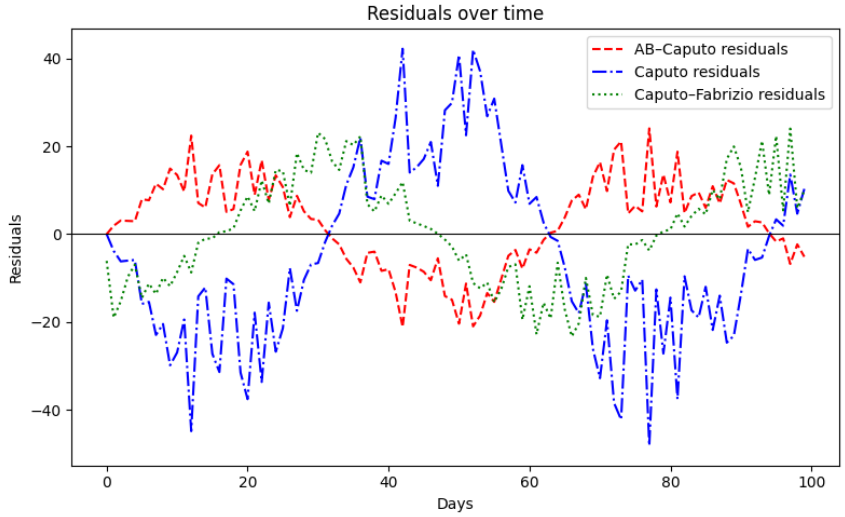

Figure 6: Residuals of the Italy model

Summary of Italy case study.. Figure 3 shows that the AB–Caputo model provides the closest match to observed incidence, reproducing the delayed peak and prolonged epidemic tail that classical Caputo and Caputo–Fabrizio derivatives fail to capture. This improved fit is confirmed in Figure 6, where AB–Caputo residuals remain consistently closer to zero across the epidemic period. Peak dynamics are summarized in Figure 4, highlighting that only the AB–Caputo model aligns with both the timing and magnitude of the observed peak. Finally, Figure 5 illustrates the robustness of the fitted parameters under changes in discretization and added noise, with narrow variability across bootstrap resamples. Taken together, these results confirm that fractional operators with non-singular kernels not only

enhance theoretical modeling but also provide reliable, data-driven insights into real epidemic dynamics.

The AB–Caputo model achieved the best fit, with fractional order $\alpha \approx 0.75$, reproducing the delayed peak and prolonged epidemic tail observed in the data. In contrast, the classical Caputo model peaked too early, and the Caputo–Fabrizio model decayed too quickly. These results confirm that fractional operators with non-singular kernels capture memory effects in real epidemiological data, such as immune persistence and behavioral adaptation.

12.3. Observations

Krasnosel'skii's fixed point theorem is used to establish positive solutions of the nonlinear fractional SIR model, and Lipschitz continuity guarantees uniqueness, offering a rigorous mathematical foundation. Additionally, the model demonstrates generalized Hyers–Ulam stability, which is crucial for epidemic prediction, as it shows that slight changes in initial conditions or parameters result in proportionately small deviations in the solution. The basic reproduction number (R_0) is calculated using the non-linear incidence function, and analytical expressions for both endemic and disease-free equilibria are obtained. The endemic equilibrium is shown to be locally stable under fractional eigenvalue conditions, and global stability is established using a Lyapunov–LaSalle method modified for the AB–Caputo derivative.

13. Conclusion

Numerical experiments showed that memory kernels strongly shape epidemic dynamics. The AB–Caputo derivative, with its Mittag–Leffler kernel, produced longer persistence and delayed peaks, better reflecting real-world memory effects such as immune persistence and heterogeneous contacts. The Adams–Bashforth–Moulton predictor–corrector scheme proved stable and reliable, confirming that fractional operators improve forecasts beyond classical models. Future work will extend this framework to SEIR/SIRS models with nonlinear features, stochastic effects, and control strategies like vaccination and isolation, while exploring integration with artificial intelligence for predictive health modeling.

Overall, the results demonstrate that fractional calculus—particularly with non singular and non local kernels like AB–Caputo—is a powerful tool for modeling complex epidemiological processes. This conclusion aligns with recent advances in fractional epidemic modeling and AI applications. Atangana [11] emphasized the role of fractional operators with non local kernels in epidemiology, while Baleanu and Atangana [13] provided new insights into infectious disease modeling. Shah et al. [16] combined neural networks with fractal–fractional analysis to predict eye disease infection, Firoozsalari et al. [17] applied deep learning to coupled fractional integro-differential systems, and Adak et al. [18] investigated fractional epidemic models using artificial deep neural networks. Together, these contributions underscore the relevance of fractional operators in modern mathematical epidemiology.

Beyond epidemiological modeling, fractional calculus is increasingly intersecting with artificial intelligence. The memory and nonlocal properties of fractional operators align

naturally with learning algorithms and neural networks, offering new pathways for predictive modeling and data driven health applications. Future work may integrate fractional epidemic models with AI frameworks to enhance forecasting, parameter estimation, and decision support.

Acknowledgement

If necessary, you can type your acknowledgement here.

References

[1] R. M. Anderson and R. M. May, *Infectious Diseases of Humans: Dynamics and Control*. Oxford University Press, 1991.
[2] H. W. Hethcote, "The mathematics of infectious diseases," *SIAM Review*, vol. 42, no. 4, pp. 599–653, 2000.
[3] W. O. Kermack and A. G. McKendrick, "A contribution to the mathematical theory of epidemics," *Proceedings of the Royal Society A*, vol. 115, no. 772, pp. 700–721, 1927.
[4] K. Diethelm, *The Analysis of Fractional Differential Equations*. Springer, 2010.
[5] M. Caputo, "Linear models of dissipation whose Q is almost frequency independent," *Geophysical Journal International*, vol. 13, no. 5, pp. 529–539, 1967.
[6] J. Liouville, "Mémoire sur quelques questions de géométrie et de mécanique," *Journal de l'École Polytechnique*, vol. 13, pp. 1–69, 1832.
[7] A. A. Kilbas, H. M. Srivastava, and J. J. Trujillo, *Theory and Applications of Fractional Differential Equations*. Elsevier Science, 2006.
[8] I. Podlubny, *Fractional Differential Equations*. Academic Press, 1999.
[9] M. Caputo and M. Fabrizio, "A new definition of fractional derivative without singular kernel," *Progress in Fractional Differentiation and Applications*, vol. 1, no. 2, pp. 73–85, 2015.
[10] A. Atangana and D. Baleanu, "New fractional derivatives with non-local and non-singular kernel: Theory and application to heat transfer model," *Thermal Science*, vol. 20, no. 2, pp. 763–769, 2016.
[11] A. Atangana, "Fractional operators with non-local and non-singular kernels: Applications to epidemiology," *Chaos, Solitons & Fractals*, vol. 102, pp. 336–348, 2017.
[12] D. Baleanu, A. Atangana, and F. Jarad, *Fractional Calculus: Models and Numerical Methods*. World Scientific Publishing, 2017.
[13] D. Baleanu and A. Atangana, "Modeling the spread of infectious diseases with fractional derivatives: New insights," *Mathematical Methods in the Applied Sciences*, vol. 40, no. 18, pp. 6394–6405, 2017.
[14] M. A. Krasnosel'skii, *Positive Solutions of Operator Equations*. Noordhoff, Groningen, 1964.
[15] K. Shah, S. Ahmad, A. Ullah, and T. Abdeljawad, "Study of chronic myeloid leukemia with T-cell under fractal-fractional order model," *Open Physics*, vol. 1, 2024, Article 20240032.
[16] K. Shah, K. U. Rehman, B. Abdalla, T. Abdeljawad, and W. Shatanawi, "Using neural network and fractals fractional analysis to predict the eye disease infection caused by conjunctivitis virus," *Fractals*, 2025, Article 2540204.
[17] A. N. Firoozsalari, H. D. Mazraeh, A. A. Aghaei, and K. Parand, "Using deep neural network in computational analysis of coupled systems of fractional integro-differential equations," *Journal of Computational and Applied Mathematics*, 2025, Article 116912.
[18] S. Adak, S. Barman, S. Jana, S. Majee, and T. K. Kar, "Study of fractional order epidemic compartmental model by using artificial deep neural networks," *Neural Networks*, 2025, Article 107944.
[19] M. A. Alqudah, K. Shah, F. Mofarreh, and T. Abdeljawad, "Mathematical modeling of psychological disease by using artificial intelligence tools," *Fractals*, 2025, Article 2550101.
[20] Eiman, K. Shah, M. Sarwar, and T. Abdeljawad, "On rotavirus infectious disease model using piecewise modified ABC fractional order derivative," *Networks & Heterogeneous Media*, vol. 1, 2024.
[21] K. A. Aldwoah, M. A. Almalahi, M. Hleili, F. A. Alqarni, E. S. Aly, and K. Shah, "Analytical study of a modified-ABC fractional order breast cancer model," *Journal of Applied Mathematics and Computing*, vol. 70, no. 4, pp. 3685–3716, 2024.

[22] Eiman, K. Shah, M. Sarwar, and T. Abdeljawad, "Modeling Virus Mutation Dynamics Using Piecewise Fractional Derivatives," *European Journal of Pure and Applied Mathematics*, vol. 18, no. 2, pp. 6053–6053, 2025.
[23] M. B. Jeelani, A. S. Alnahdi, M. S. Abdo, M. A. Abdulwasaa, K. Shah, and H. A., "Mathematical modeling and forecasting of COVID-19 in Saudi Arabia under fractal-fractional derivative in Caputo sense with power-law," *Axioms*, vol. 10, no. 3, Article 228, 2021.
[24] E. Y. Salah, B. Sontakke, M. S. Abdo, W. Shatanawi, K. Abodayeh, and M. D. Albalwi, "Conformable Fractional-Order Modeling and Analysis of HIV/AIDS Transmission Dynamics," *International Journal of Differential Equations*, vol. 2024, no. 1, Article 1958622, 2024.
[25] M. Khan and A. Atangana, "Analytical study of transmission dynamics of 2019-nCoV pandemic via fractal fractional operator," *Results in Physics*, vol. 24, 104045, 2021.
[26] T. Abdeljawad, M. S. Abdo, F. Jarad, and K. Shah, "An Analytical Study of Fractional Delay Impulsive Implicit Systems With Mittag-Leffler Law," *Applied and Computational Mathematics*, vol. 22, no. 1, pp. 34–44, 2023.
[27] M. B. Jeelani, A. S. Alnahdi, M. S. Abdo, M. A. Almalahi, N. H. Alharthi, and K. Shah, "A generalized fractional order model for COV-2 with vaccination effect using real data," *Fractals*, vol. 31, no. 4, Article 2340042, 2023.
[28] W. M. Liu, H. W. Hethcote, and S. A. Levin, "Dynamical behavior of epidemiological models with nonlinear incidence," *Mathematical Biosciences*, vol. 82, no. 2, pp. 121–147, 1987.
[29] G. Chowell, P. W. Fenimore, M. A. Castillo-Garsow, and C. Castillo-Chavez, "SARS outbreaks in Ontario, Hong Kong and Singapore: The role of diagnosis and isolation as a control mechanism," *Journal of Theoretical Biology*, vol. 224, no. 1, pp. 1–8, 2009.
[30] Presidenza del Consiglio dei Ministri – Dipartimento della Protezione Civile. *COVID-19 Italia – Dati e monitoraggio*. 2020. Available at: https://www.protezionecivile.it
[31] Rami Krispin. *covid19Italy: The 2019 Novel Coronavirus COVID-19 Italy Dataset*. 2021. R package on CRAN. Available at: https://cran.r-project.org/package=covid19Italy
[32] Our World in Data. *Coronavirus Pandemic – Italy Country Profile*. 2025. Available at: https://ourworldindata.org/coronavirus/country/italy
[33] F. Alshammari et al., "Fractional Epidemic Systems with Mittag–Leffler Kernels," *Fractal and Fractional*, vol. 9, no. 11, p. 10690, 2023. doi:10.3390/fractalfract9110690
[34] F. Alshammari and A. Atangana, "Fractal–Fractional Operators in Epidemiological Dynamics," *Fractal and Fractional*, vol. 9, no. 11, p. 10709, 2023. doi:10.3390/fractalfract9110709
[35] S. Adak, S. Barman, S. Jana, S. Majee, and T. K. Kar, "Modelling and analysis of a fractional-order epidemic model incorporating genetic algorithm-based optimization," *Journal of Applied Mathematics and Computing*, vol. 71, pp. 901–925, 2025. doi:10.1007/s12190-024-02224-y
bibitemShafqat2025 R. Shafqat, S. M. Alamry, and A. Alsaadi, "Analysis and simulation of a normalized Caputo–Fabrizio fractional SEIR epidemic model," *AIMS Mathematics*, vol. 10, no. 10, pp. 24712–24729, 2025. doi: 10.3934/math.20251095